Computers and Electronics in Agriculture 212 (2023) 108126

Contents lists available at ScienceDirect

Computers and Electronics in Agriculture

journal homepage: www.elsevier.com/locate/compag

Original papers

A planning strategy for sprinkler-based variable rate irrigation

Gabriele Penzotti *, Dario Lodi Rizzini, Stefano Caselli

CIDEA, University of Parma, Parma, Italy

ARTICLE INFO

Keywords:
Precision agriculture
Variable rate irrigation
Agricultural automation
Smart services
Remote sensing

ABSTRACT

Automated variable rate irrigation (VRI) is one of the frontiers for sustainable water use in agriculture. In this paper, we describe a planning procedure for self-propelled rain gun sprinklers, a type of equipment largely used in irrigation of open field crops thanks to its relatively low cost and easy deployment in multiple sites. The sprinkler is commanded by an information system which acquires data from remote sensors (satellite), processes vegetation indices and spatial maps describing the water need of the crop, and computes a VRI prescription map for a specific field, i.e. the water quantity to be supplied to each field sub-area. The VRI prescription map is used to compute the motion commands for a rain gun system pulled by a hose reel. The procedure is based on a sprinkler model, has been validated by simulation, and is fully automated. Experiments have shown the precision in water distribution achievable with software-controlled sprinklers and effective planning strategies.

1. Introduction

Precise, site-specific irrigation is a major challenge and critical task to achieve efficient use of water resources in farming as well as to meet sustainability goals. Advancement in technology has made viable variable rate irrigation (VRI) (Evans et al., 2020; O'Shaughnessy et al., 2019), with clear potential economic, environmental, and agronomic advantages. Yet, the widespread application of VRI is hindered by the complexity and cost associated with the deployment of new or upgraded irrigation equipment.

Among the different irrigation techniques, sprinkler-based irrigation using self-propelled machines, either with linear motion or with center pivot, is a widespread practice, especially in massive production farming involving large-scale crops (Evans et al., 2020; Mostafa and Derbala, 2013). Indeed, sprinkler irrigation covers a significant fraction of irrigated land worldwide (e.g., above 60% in Europe and above 40% in Northern America) (Pereira and Gonçalves, 2018). Mobile rain gun irrigation sprinklers, investigated in this work, are among the most widespread machines in open field irrigation, thanks to their relatively low cost and easy deployment by the farmer in multiple fields. The development of techniques enabling automatic monitoring, planning and control of machines equipped with VRI capabilities, including sprinkler-based machines, can have therefore a significant impact toward water use efficiency and sustainability (Abioye et al., 2020; Evans et al., 2020).

In the last two decades, a number of Decision Support Systems (DSS) (Bergez et al., 2012; Moreira Barradas et al., 2012; Rinaldi and He, 2014; O'Shaughnessy et al., 2015; Adeyemi et al., 2018) have been proposed to schedule VRI. These DSS are designed for different irrigation techniques, often targeting specific crops, and operate at different spatial resolution (e.g. entire field or site-specific). They cope with spatial and temporal variability using various amount and type of prior static knowledge (e.g. about soil variability) and sensor-acquired data (e.g., weather or vegetation information). The DSS in Bergez et al. (2012) and in Moreira Barradas et al. (2012) provide schemes for space decomposition at different scales, from regional to irrigation block to field partitions, but do not include automatic acquisition of sensor measurements from the crop nor support planning of VRI. Haghverdi et al. (2016) investigate the potential of site-specific irrigation with optimized water production functions and adapt the resulting irrigation prescriptions to large center pivot machines. However, the degree of automation of the data flow from the irrigation prescription to the programming of the machine is unclear. Moreover, the approach does not consider other types of irrigation equipment. Li et al. (2020) point out the importance of using a sensor network including remote sensing, in-site and IoT devices to enable precision irrigation with sprinklers. However, they do not provide the procedures and models to transform irrigation prescription maps into irrigation plans suitable for actual irrigation equipment, and specifically for self-propelled rain gun sprinklers.

In general, DSS allow accurate assessment of the proper, site-specific water needed by the crop, and hence are a key step toward efficient use of water. Their main limitation lies in the lack of integration between

* Corresponding author.
E-mail address: gabriele.penzotti@unipr.it (G. Penzotti).

https://doi.org/10.1016/j.compag.2023.108126
Received 24 January 2023; Received in revised form 3 May 2023; Accepted 2 August 2023

the information system and the automated irrigation equipment available to the farmer. Full machine-to-machine operation requires to take into account the farming geometry and the actual differential irrigation capabilities of the machine.

Studies dealing with physical modeling of linear sprinklers (Carrión et al., 2001; Li et al., 2015; Ouazaa et al., 2014; Ferreira Borges and Teixeira de Andrade, 2021; Hua et al., 2022) focus on water distribution patterns obtained with different shapes and sizes of the nozzle to improve water distribution uniformity in fixed position and do not investigate the effectiveness of irrigation in motion, nor they consider the application to VRI. While accurate sprinkler models are required to measure and improve machine performance, such analysis does not cope with water distribution on the farming field and has limited applicability in sprinkler motion planning.

There are few works investigating the water distribution on farming fields achieved by irrigation systems like center pivot systems (McCarthy et al., 2010) or movable rain gun sprinklers (Ghinassi, 2010; Miodragovic et al., 2012), either through simulation or experimental assessment. Such studies enable prediction and even planning of the machine motion, often aimed at uniform water distribution rather than at informed and sensor-guided VRI.

In this paper, we propose a planning procedure for the motion of a rain gun sprinkler enabling automated irrigation according to the best approximation of a *VRI prescription map* generated by a DSS. Indeed, the potential use of rain guns for VRI is deterred by the difficulty for the farmer of programming non-uniform water distributions. The automatic execution of irrigation through a programmable actuator better guarantees that the correct quantities of water are properly supplied to the crop. To our knowledge, there are no automated systems connecting high level prescription maps to rain gun actuators for VRI. Moreover, given the extensive use of movable rain gun sprinklers, this approach can have a beneficial impact toward widespread application of VRI.

The planning procedure for rain gun sprinklers reported in this paper has been developed in the frame of project POSITIVE[1] (Amoretti et al., 2020; Penzotti et al., 2022), whose information system and processing pipeline are described in the next section. The outcome has been assessed through both simulation and experiments. Simulation is based on a purposely-designed distribution model, reported in the paper, that abstracts from hydrodynamic aspects and allows offline prediction of water distribution. Field experiments have been performed in a farm using an advanced industrial rain gun, the *Elektrorain* system manufactured by the company SIME Srl, Italy.[2] For this purpose, a software module has been developed to control the rotation speed and angle limits of the sprinkler head according to the planned motion, and the rain gun control unit has been directly interfaced to the POSITIVE information system.

In summary, the contributions of this study are the following:

1. We illustrate a system for computation of a field-specific irrigation plan suitable for rain gun sprinklers starting from the prescription of an irrigation DSS.
2. We propose an algorithm as well as a system physical model for planning the motion of a rain gun sprinkler in order to achieve differential irrigation on field partitions.
3. We report the implementation and testing of the planning algorithm with an actual sprinkler in a field experiment and in simulation.

2. Overview of the irrigation system

2.1. Approach to planning VRI with rain gun sprinklers

Rain guns are usually connected to hose reels by a pipe and are moved by wrapping the hose while sprinkling water on the field. During the backward motion, the rain gun head rotates in order to distribute water in the desired directions. Recently, advanced rain guns and hose reels can be controlled through software interfaces in order to automate irrigation. The planning algorithm described in this paper controls the rotation speed and angle limits of the sprinkler and the reeling speed of the hose reel to which the rain gun is attached. The rain gun supplies water while pulled by the hose reel, thereby irrigating a *pull area*. Hence, the reported procedure allows differentiation of the water quantity distributed within each pull area by planning the sprinkler motion. The pull area can be partitioned both longways, into multiple segments, and crosswise, into left and right regions.

Although VRI prescription maps can be obtained by feeding a DSS with remote (e.g. satellite-based vegetation maps) or local (e.g. distributed soil moisture data) sensor information, these maps do not translate directly into the differential irrigation which can be actually applied by available equipment. Hence, in this paper we develop a planning system to map a *generic VRI map*, possibly articulated into $10\ \text{m} \times 10\ \text{m}$ pixels corresponding to satellite-derived Vegetation Index (VI) maps, into a proper partitioning in *sub-regions* which can be applied by a specific irrigation machine, taking into account its features and constraints as well as its position and motion direction in the field (in general not aligned with satellite-based maps). The proposed planning algorithm computes the variable retraction velocity of the sprinkler and the rain gun orientation limits over the time so as to deliver water to the crop according to the most accurate, feasible approximation of the processed VRI prescription map.

2.2. POSITIVE information system

Project POSITIVE (Amoretti et al., 2020; Penzotti et al., 2022) has tackled precision irrigation over large regions by transforming multispectral images from Copernicus satellites and data from field sensors into high resolution crop- and terrain-specific irrigation prescription maps. Planning actuation of the prescription map via a rain gun sprinkler is one of the open protocols developed within the project.

In POSITIVE the irrigation prescription map for each registered plot is provided by the IRRIFRAME[3] agronomic DSS (Mannini et al., 2013), and relies on a number of information flows and knowledge sources, including plot geometry (called polygon), soil structure and map, crop management information (crop type, seed or plant date, etc.), crop development model, history of precipitations and irrigations, data from sensors in the plot (if any), and weather forecasts.

IRRIFRAME is available in most Italian regions and managed by the national association of water reclamation consortia under the technical guidance of CER (Canale Emiliano Romagnolo).[4] The service is freely accessible by registered farmers and provides on a daily-basis updated agronomic advice for registered fields and crops. It provides an irrigation and fertigation calendar trading off crop requirements with sustainable management of water and other resources (e.g., pesticides and nutrients), thus reducing the impact of cultivation. IRRIFRAME maintains a data record of each registered field or plot and updates such record with any information provided by the user and with the measurements provided by on-field and remote sensing data. In POSITIVE, the IRRIFRAME data record of each registered plot has been enriched with the Normalized Difference Vegetation Index (NDVI) and Enhanced Vegetation Index (EVI) maps (Huete et al., 2002), computed from

[1] http://www.progettopositive.it.
[2] https://www.simeirrigation.it.
[3] https://www.irriframe.it.
[4] https://www.consorziocer.it.

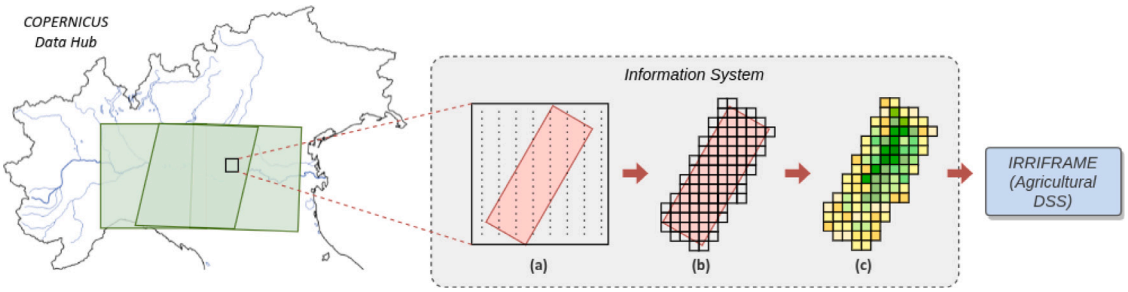

Fig. 1. POSITIVE data flow to upload satellite-sensed data to the IRRIFRAME DSS. (a) Satellite products are obtained for large areas via the Copernicus Hub API, cropping out the area of interest. (b) Pixels that carry information on the polygon are extracted; data verification and cleaning operations for presence of artifacts, edge effects and more are applied. (c) NDVI and EVI maps are computed from the cleaned images, formatted, and uploaded in IRRIFRAME.

Sentinel-2 products. Custom information services for data processing and storage have been implemented in POSITIVE to manage the flow of Sentinel-2 data to IRRIFRAME. An overall view of this process, repeated each time there is a valid Sentinel-2 sampling, is shown in Fig. 1.

The water application depth is computed in IRRIFRAME via an evapotranspiration model based on crop coefficient. This default prescription has been enriched in POSITIVE using the NDVI and EVI maps, which enable a continuous recalibration of the prescription based on satellite revisit times (typically every 5 days). Moreover, for large-scale crops the basic irrigation prescription is generalized into a VRI prescription map at the resolution (10 m) of Copernicus multispectral imagery.

Although producing a valid irrigation map is the output of a complex DSS, in this paper we focus on the exploitation of satellite-based data and related VI to enable VRI where appropriate. In the pipeline encompassed by POSITIVE, irrigation machines like movable rain gun sprinklers, linear spray booms or center pivot systems are bound to execute the water application depth maps.

2.2.1. Data-driven irrigation

Data-driven irrigation systems comprise two main modules: an information system and one or more actuators for irrigation.

- *Information System*. The information system coordinates the acquisition of all data and information required to produce a valid irrigation prescription. A key component for smart irrigation is the specialized DSS. The final output of the information system is the *irrigation prescription* presented as a *map*, associating to each partition of a field the water supply required by the crop. The field surface can be partitioned in several ways: for example, satellites provide data about a field with a given surface resolution, whereas the same field is divided into tracks according to the physical characteristics of the specific irrigation equipment (e.g., the range of the rain gun sprinkler). Moreover, the irrigation equipment used in a field can change over time, so partitioning and mapping among partitions must be configurable. The map must be adapted to the required field partitioning when delivered to the farmer or to the irrigation system.
- *Actuators for Irrigation*. The information system can automatically deliver a VRI water depth map to advanced irrigation machines equipped with a suitable control unit. There are different types of sprinkler-based irrigation machines that can receive and apply VRI maps. In this work, we focus on rain gun sprinklers towed by a hose reel winch.

The components of the information system are described next according to the data flow shown in Fig. 2.

VRI requires a differentiated irrigation prescription map for different areas of the plot based on the localized need of the crop. A standard approach (Brown, 2015) is to retrieve information from the remote sensing activities of the Copernicus program, chiefly the *products* made available by Sentinel-2 satellites. Sentinel-2 data are available in the form of multispectral images of large geographical areas, composed in 13 spectral bands and with different resolutions. Products are provided in Cartesian raster format, in which each pixel represents a square plot of land with a side equal to the resolution.

For the areas of interest, the information system retrieves and stores the products at each new transit of the satellites. These products are processed in terms of VI maps referred to a plot, and then delivered to IRRIFRAME, which provides site-specific agronomic information and irrigation and fertigation prescriptions for registered fields and crops (Mannini et al., 2013). In the experiment reported in this paper, the well-known NDVI computed from the Sentinel-2 products has been adopted. This approach is extensible to other appropriate VI or information derived from sensing activities.

The spectral bands needed for computing the NDVI map are provided by Sentinel-2 products at the maximum resolution of 10 m. This resolution is adequate for many open field crops (corn, tomato, soybean, etc.) in medium–large plots, where the plot is covered by a high number of samples. Conversely, very small plots are too limited and unsuitable for VRI based on satellite data. Other operations required for computation of an NDVI map suitable for the DSS include verification and cleaning of the Sentinel-2 products, such as outlier removal, filtering around the edges of the plot for mitigation of artifacts in the images (e.g., roads and buildings), and coordinate system transformation.

In addition to the processed NDVI map, IRRIFRAME exploits a wealth of information to compute the water irrigation prescription for the plot, including crop, soil, and weather information. At the end of the process, a spatially-variable water application map is available, i.e. a map that associates to each field cell the recommended water application to be supplied. Usually, the map is provided in the form of a tessellation of square cells $C_1, \ldots, C_k$, where the size of each C_j is $10\ \text{m} \times 10\ \text{m}$ exploiting the resolution of Sentinel-2 images. The application depth of a cell C_j is the quantity of water V_j expressed in the form of the total water volume for the surface C_j or as the average water application depth per surface point.

The final step is transformation of the irrigation prescription map into irrigation machine commands. This operation is strongly dependent on the available actuators. Irrigation machines may be equipped with communication interfaces to receive commands and transmit data to the information system. In such case, the VRI process can be fully automated.

In this paper, we report the interfacing of the POSITIVE information system with a movable rain gun sprinkler via a custom communication protocol defined by the manufacturer. The rain gun can receive commands in real-time and hence be driven by a software application. Special-purpose services have been implemented in order to translate the irrigation prescription map into low-level commands, as the *Elektrorain* rain gun is not natively configured to operate VRI.

2.2.2. Actuators for irrigation

Electronically-controlled actuators are mandatory to achieve automatic irrigation according to the water application depth provided by the information system. Movable rain gun sprinklers comprise:

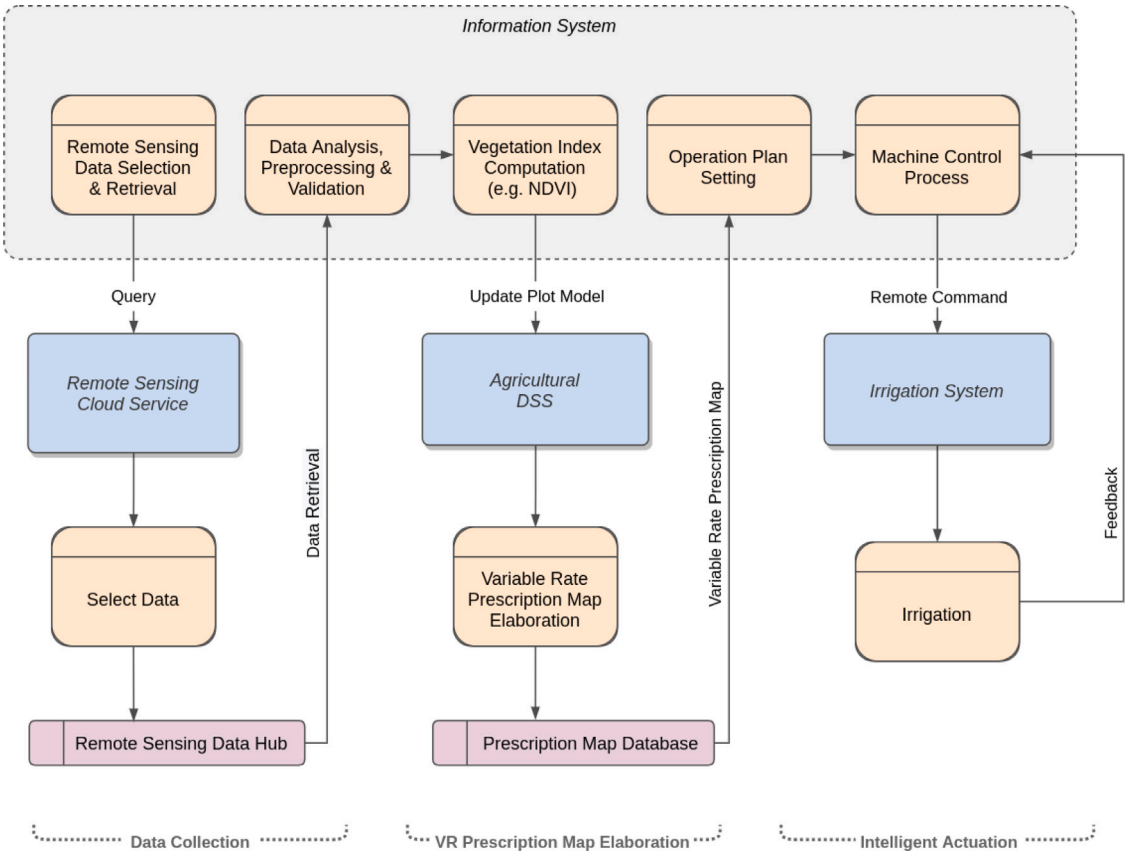

Fig. 2. Data flow of the application for sprinkler-based VRI. The main activities are acquisition of remote sensing data (possibly integrated by local sensor data), acquisition of the water application map, actuation of data-driven irrigation. Data acquisition and model update are performed continuously.

- a self-winding towing machine (hose reel) positioned at one side of the plot and connected to the water supply via a pump;
- a towed trolley with a rain gun or cannon, mounted as a rotating arm, which irrigates by sprinkling (see Fig. 3).

Initially, the trolley is transported away from the reel on the other side of the irrigated plot by means of a tractor, unrolling the feeding-towing hose. During irrigation, the towing machine rolls up the hose, thereby drawing to itself the sprinkler trolley. We refer to this type of movement as a *pull*. To each pull corresponds a rectangular wet region at the end of the irrigation. The quantity of water delivered depends on the dimensional characteristics of the machines, on the pressure with which the system is fed, and on the speed commanded to the trolley, called *retraction speed*. In order to apply VRI as proposed in this paper, the actuators must implement advanced mechanical and electronic features as summarized below.

Mechanical features. Both the hose reel and the rain gun must have the ability to differentiate the amount of water released along the pull, changing some of the parameters.

- The hose reel must be able to modify the retraction speed during execution, thus slowing down the movement of the trolley where a larger supply of water is required.
- The rain gun must be able to modify the rotation speed and/or the start and end stroke angles. Indeed, recent rain gun models provide such feature, even though it was designed to increase the uniformity of the sprinkled water or to avoid wetting unwanted areas on the edge or inside the plot. Through appropriate modeling and programming, as reported in this paper, the feature can be exploited to differentiate the quantity of water delivered transversely to the pull direction.

Other parameters, such as the water flow, are difficult to modify and are usually considered non-changeable in real-time.

Electronic features. The irrigation system must be able to receive and follow an irrigation plan, that is, to memorize and effect changes to the parameters described above on the basis of the different water application depths required along the pull. This programmability can be static or dynamic, i.e. it can be set only before irrigation or it can be continuously corrected based on real-time sensor feedback or commands. In this case, a remote communication capability on the part of the machines is required.

The SIME Elektrorain rain gun sprinkler provides the mechanical, electronic and communication features described above and hence has been used as a reference and for the experiments reported in this paper. However, the proposed irrigation planning procedure is quite general and can be applied to any rain gun with the required features.

3. Model for sprinkler-based irrigation

This section provides a simplified model for mobile rain gun sprinklers and for the irrigation process. The model will be used for planning irrigation according to a VRI prescription map.

3.1. Sprinkler state model

Sprinkler irrigation is achieved by retracting the rain gun, which is commanded by reeling the hose, and by rotating the rain gun head during the retract motion. Assuming water flow approximately constant during irrigation, water distribution depends on the changes in position and orientation of the rain gun in the course of irrigation, in other words by the state of the sprinkler.

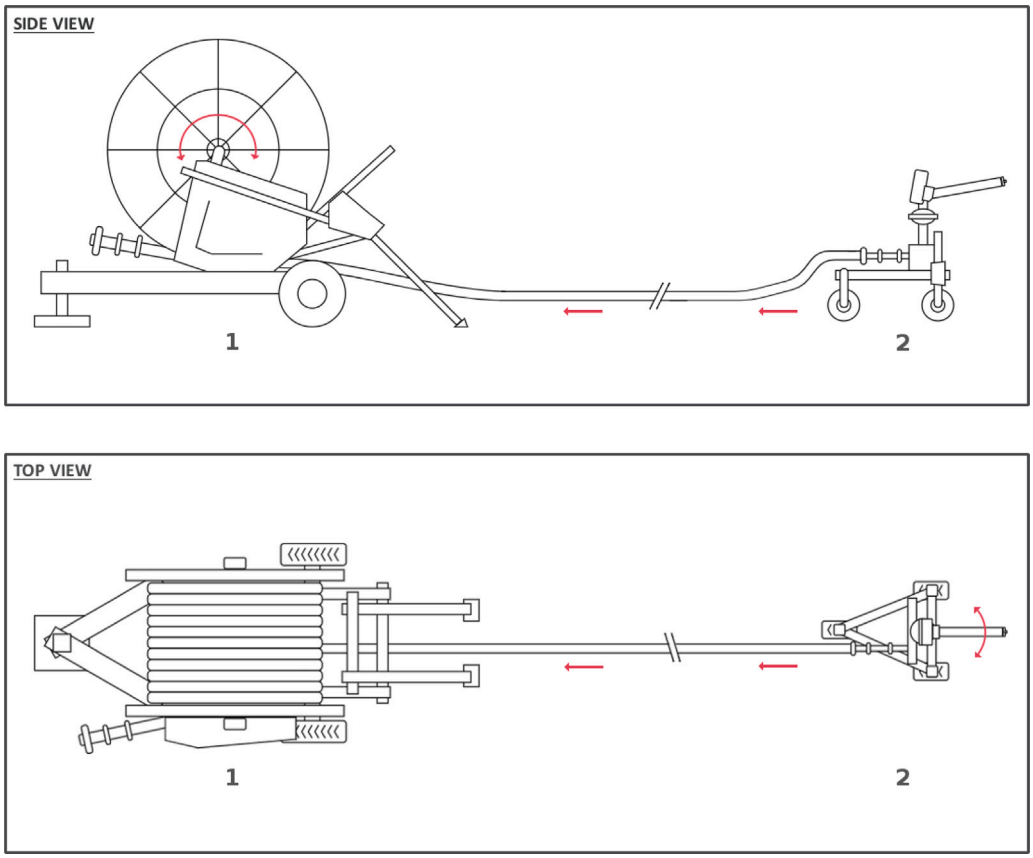

Fig. 3. Schema of the irrigation system, consisting of a hose reel (1) and a rain gun cannon (2). The dynamics of the actuators are schematized by red arrows.

The state variables represent the position and orientation of the modeled sprinkler in the world. Geographic information systems describe the position of irrigation machines and fields according to geographic spherical coordinate systems, but in this context a planar Euclidean reference system is more convenient. We assume that the reference frame *local* $\{L\}$ is placed on the ground surface that we approximate with a plane, and that the position and orientation of the *sprinkler* frame $\{S\}$ is given by pose vector $[q_x, q_y, q_\theta]^\top$ representing the transformation matrix ${}^L_S\mathbf{T}$. Without losing generality, we assume that the *pull direction* is the same of axis x of $\{L\}$ and, hence, $q_y = 0$. It is reasonable to assume the orientation of the sprinkler frame consistent with the wrapping direction, i.e. $q_\theta = 0$. The orientation of the rotating head of the sprinkler, which is responsible for the water flow direction, is described by angle q_φ. Thus, the state vector of the sprinkler is $\mathbf{q} = [q_x, q_y, q_\theta, q_\varphi]^\top$, which can be reduced to the components $\mathbf{q} = [q_x, q_\varphi]^\top$ since for most problems $q_y = 0$ and $q_\theta = 0$. It will be clear from context whether the symbol $\mathbf{q}$ refers to the full or the reduced state vector.

The evolution of the sprinkler state is described by the simple equations

$$\dot{q}_x = v \tag{1}$$

$$\dot{q}_\varphi = \omega \tag{2}$$

A single irrigation pull starts with the sprinkler in position $q_x = l_p - r$, where l_p is the length of the pull rectangle and r is the range of the water flow. Then, it is pulled by the hose reel and moves with speed $v = -v_w$, where the retraction velocity $-v_w$ is negative since the motion versus is contrary to the axis x of frame $\{L\}$. The rotating head of the sprinkler changes its orientation between two extreme angles φ_i and φ_f and the rotation speed is ω. In the case of uniform irrigation on all the field, the input $\omega(t)$ is a step function for every sweeping cycle $k = 0, 1, \ldots$

$$\omega(t) = \begin{cases} \omega_s & k\,T_s \leqslant t < \left(k + \frac{1}{2}\right)\,T_s \\ -\omega_s & \left(k + \frac{1}{2}\right)\,T_s \leqslant t < (k+1)\,T_s \end{cases} \tag{3}$$

where ω_s is the constant sweeping speed, $T_s = 2(\varphi_f - \varphi_i)/\omega_s$ is the sweeping time and the orientation in $q_\varphi(0) = \varphi_i$. The above command can be reformulated with respect to the sprinkler orientation as

$$\omega(t) = \begin{cases} \omega_s & -\varphi_i \leqslant q_\varphi(t) < 0 \\ -\omega_s & 0 \leqslant q_\varphi(t) \leqslant \varphi_f \end{cases} \tag{4}$$

This second form divides the interval according to another state variable and is more convenient in many computations.

3.2. Irrigation model

The hydraulic model adopted here is simplified. We assume that the water pushed in the sprinkler has constant pressure p (Pa), constant volumetric flow rate f $(\mathrm{m}^3/\mathrm{s})$ and constant range r (m). The range is defined as the distance between the sprinkler center and the point where flowing water concentration is maximum. We will propose in Section 5 a distribution function for application rate that approximates a more accurate hydrodynamic model. However, this section avoids the choice of a specific distribution by reasoning on the average water spilled on a field area. The model assumes that the maximum range r and the application rate distribution of the sprinkler rain gun are negligible compared with the longitudinal length l_p of the field (or the longitudinal length l_x of a field sector, if the field is split longitudinally).

The irrigation area reached by the sprinkler in a single pull is abstractly defined as a *pull rectangle*. The length of the pull rectangle is equal to l_p, which is the length of the path traveled by the sprinkler

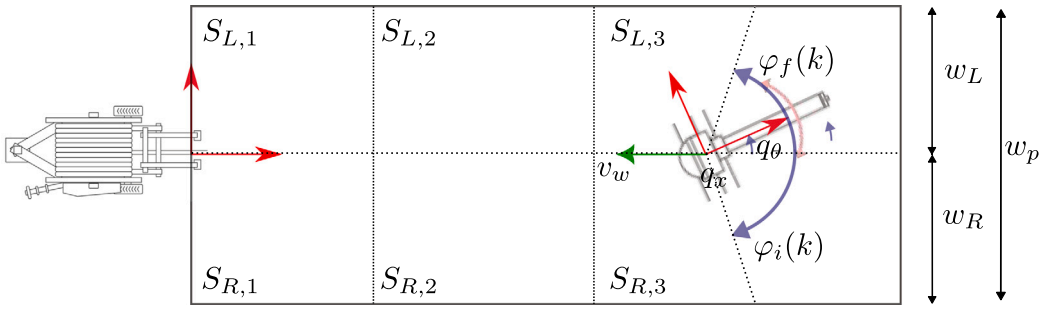

Fig. 4. Illustration of sprinkler state variables and of field parameters. In this example, the field is partitioned into 3 longitudinal and 2 transversal (left and right) sectors.

when pulled by the hose reel. Its width w_p depends on the angle interval $[\varphi_i, \varphi_f]$ covered by the rotating head of the sprinkler

$$w_p = r \sin \varphi_f - r \sin \varphi_i \tag{5}$$

If $\varphi_i = -90$ deg and $\varphi_f = +90$ deg, then $w_p = 2\ r$, i.e. the width is the double of the sprinkler range. On average, the water volume $V_{t_0,t_1} = \int_{t_0}^{t_1} f\ d\tau$ supplied in a time interval $[t_0, t_1]$ is distributed by the sprinkler retracting with wrapping speed v_w on the surface with area equal to

$$S_{t_0,t_1} = w_p \int_{t_0}^{t_1} v_w\ d\tau \tag{6}$$

The surface S_{t_0,t_1} represents the area reached by the sprinkler jet, even though the water distribution is possibly uneven. On average, the water application depth is

$$h_a = \frac{V_{t_0,t_1}}{S_{t_0,t_1}} = \frac{f}{w_p\ v_w} \tag{7}$$

The above equality is exact when both f and v_w are constant over interval $[t_0, t_1]$, i.e. $V_{t_0,t_1} = f\ (t_1 - t_0)$ and $S_{t_0,t_1} = w_p\ v_w\ (t_1 - t_0)$. The supplied water per unit surface h_a is an average value achieved through changes of the sprinkler position (q_x) and sprinkler head orientation (q_φ).

When modeling the instantaneous water distribution of a rain gun as in Section 5, we have to use the *application rate*, which is the time derivative of h.

This simple model can be used to specify the water volume supplied to different areas. For example, the pull rectangle can be split longitudinally along the pull direction x and transversely along the orthogonal direction y. The regions corresponding to the longitudinal partition of the pull rectangle are called *sectors* S_j. Each sector S_j is further partitioned into left $S_{L,j}$ and right $S_{R,j}$ sub-sectors with respect to the sprinkler retraction line. The total water volume supplied on sector $S_j = S_{L,j} \cup S_{R,j}$ depends on the retraction speed v_w (i.e. on the time the sprinkler jet falls on the field with constant volumetric flow rate f), but the water supplied to each sector $S_{L,j}$ and $S_{R,j}$ can be diversified according to the time the sprinkler is directed on the left or on the right. The sprinkler state variables are illustrated in Fig. 4. We focus on the precision irrigation of the left and right sub-sectors that can be replicated separately on each sector under the hypothesis that longitudinal transition between contiguous sectors has negligible effect on irrigation.

Let T_S be the *sweeping time*, i.e. the time required by the sprinkler head to visit twice the angle interval $[\varphi_i, \varphi_f]$. The sweeping time T_S is also the period of the system. Let T_L and T_R be the amount of T_S s.t. the sprinkler is directed to respectively the left and the right sub-sectors, $T_S = T_L + T_R$. The total volume of water V_S is then split into $V_L = V_S\ T_L/T_S$ and $V_R = V_S\ T_R/T_S$, and using Eq. (7) the water application depths on left and right are respectively

$$h_L = \frac{f\ T_L}{w_L\ v_w\ (T_L + T_R)} \qquad h_R = \frac{f\ T_R}{w_R\ v_w\ (T_L + T_R)} \tag{8}$$

where the $w_L = r \sin \varphi_f$ and $w_R = -r \sin \varphi_i$ are the widths of respectively the left and the right sectors, and $w_p = w_L + w_R$. If symmetric angle values $\varphi_i = -\alpha$ and $\varphi_f = \alpha$ are assigned, then $w_L = w_R = r\ \sin \alpha$. In such symmetric case, the ratio between left and right application depths depends straightforwardly on the left and right times as

$$\frac{h_L}{h_R} = \frac{T_L}{T_R} \tag{9}$$

There are different ways to control T_L and T_R and two of them are discussed in Section 4. The ratio of T_L and T_R only depends on the state variables of the rain gun like its rotation speed or the initial and final rotation angles. Conversely, the average water application rate is a function of retraction speed v_w, which is controlled by the hose reel towing machine. In the symmetric case, the average application depth on a sector is $h_a = (h_L + h_R)/2$. The pull speed needed to achieve the required average h_a in a sector is derived from Eq. (7) as

$$v_w = \frac{2\ f}{w_p\ (h_L + h_R)} \tag{10}$$

Thus, the sprinkler commands for controlling the application depths on sub-sectors are computed from Eqs. (9) and (10). The proposed model holds under the hypothesis that the target values of h_L and h_R as well as the retraction speed v_w smoothly change in longitudinal direction. Moreover, full variable rate irrigation requires control and communication of both the rain gun sprinkler and the towing machine that often have different manufacturers. In this paper, we focus only on the former component.

4. Planning for precise irrigation

This section presents two policies for computing irrigation commands to achieve different application rates h_L and h_R in left and right sub-sectors with respect to the pull direction of the sprinkler. The first method is based on differential angular speeds of the sprinkler. The second method is based on the manipulation of initial and final angles of the sprinkler. The second method is more consistent with the requirements of real irrigation scenarios and is therefore better described.

Setting differentiated angular speeds. The total water volume $V = f\ \Delta t$ can be split in the two sub-sectors according to the time the sprinkler is directed toward each of them according to Eq. (8). Such goal could be achieved by setting different rotation speeds ω_L and ω_R respectively on the left and on the right sectors

$$\omega(\mathbf{q}, \dot{\mathbf{q}}) = \begin{cases} \omega_L & 0 \leqslant q_\varphi \leqslant \varphi_f \text{ and } \dot{q}_\varphi > 0 \\ \omega_R & \varphi_i \leqslant q_\varphi < 0 \text{ and } \dot{q}_\varphi > 0 \\ -\omega_L & 0 \leqslant q_\varphi \leqslant \varphi_f \text{ and } \dot{q}_\varphi < 0 \\ -\omega_R & \varphi_i \leqslant q_\varphi < 0 \text{ and } \dot{q}_\varphi < 0 \end{cases} \tag{11}$$

where $\omega_L, \omega_R > 0$. In each sweep, the time intervals in which the sprinkler is directed toward the left and right sectors are respectively $T_L = -2\varphi_i/\omega_L$ and $T_R = 2\varphi_f/\omega_R$. The non-continuous staircase function in Eq. (11) is just a setpoint and the real speed depends on

the dynamics of the system. It would be more realistic to set trapezoid or even parabolic command functions for transitions from ω_L to ω_R and vice versa, but this paper will not address this approach. In the symmetric case, the ratio of application depths of Eq. (9) is related to the angular speeds in the left and the right sub-sectors according to

$$\frac{h_L}{h_R} = \frac{T_L}{T_R} = \frac{(\varphi_f/\omega_L)}{(\varphi_f/\omega_R)} = \frac{\omega_R}{\omega_L} \tag{12}$$

Thus, different irrigation of the left and right sub-sectors can be achieved by setting different values of the rotation speed, ω_L and ω_R.

However, setting non-uniform values of the gun rotation speed incurs several disadvantages from a crop perspective. The jet range slightly changes during rotation so that the adoption of different speeds may result into unequal coverage of irrigation areas. The transition between setpoints ω_L and ω_R is not immediate. Moreover, a slower rotation speed implies that the sprinkler jet falls for longer time on a specific area, i.e. it applies force on the same plant which could be excessive for some crops.

Setting differentiated angular trajectories. An alternative modulation of water flows in the left and right sub-sectors is achieved by dynamically changing φ_i and φ_f, while keeping a constant value for ω. This approach should be preferred since it reduces uneven water distribution, accelerated drops, and potential damage of the crop. Let k be the index of the sweeps of the sprinkler. For each sweep, the extreme angles $\varphi_i(k)$ and $\varphi_f(k)$ can be set. In the course of n sweeps, the total sweeping times of the left and right sub-sectors are

$$T_L = \sum_{k=1}^{n} \frac{2\varphi_f(k)}{\omega} \qquad T_R = \sum_{k=1}^{n} \frac{-2\varphi_i(k)}{\omega} \tag{13}$$

For sake of uniformity, it would be convenient to have sweeps covering all the available angle interval, i.e. $\varphi_i(k) \in \{0, -\alpha\}$ and $\varphi_f(k) \in \{0, \alpha\}$. With the standard choice $\alpha = \pi/2$, at each sweep k we may have a *complete sweep* covering both left and right, or a *half-sweep* either to the left or to the right. Let $c_L, c_R \in \{0, \dots, n\}$ be the counters of left and right half-sweeps in a sequence of n sweeps. Under these hypotheses, Eq. (13) has the simpler expression

$$T_L = \frac{2\alpha}{\omega}\, c_L \qquad T_R = \frac{2\alpha}{\omega}\, c_R \tag{14}$$

If the times T_L and T_R depend on the integer counters c_L and c_R, the ratio of the application depths in Eq. (9) is also constrained by the feasible values of the discrete variables c_L and c_R.

The total irrigation time of the sprinkler on a longitudinal sector of length l_x is equal to l_x/v_w, where v_w is the pull speed set for the sector as in Eq. (10). Such sector time may not correspond exactly to the time required for N sweeps given by the sum of T_L and T_R, since these times refer to complete half-sweeps on the left and right sub-sectors. Hence, there is a residual time T_δ spent during transition to the next sector. Thus, the total irrigation time on a sector of length l_x is

$$T_L + T_R + T_\delta = \frac{l_x}{v_w} = \frac{l_x\, w_p\, (h_L + h_R)}{2\, f} \tag{15}$$

The desired value is $T_\delta = 0$, but the chosen simplified control of sprinkler rotation makes T_L and T_R function of integer variables (the half-sweep counters) as discussed in the following.

Both Eqs. (9) and (15) constrain the times T_L and T_R and the desired application depths h_L and h_R. Eq. (9) can only be approximated, since T_L and T_R depend on discrete variables. Thus, the planning problem can be formulated as

$$\frac{h_L}{h_R} = \frac{T_L}{T_R} = \frac{c_L}{c_R} + r_\delta \tag{16}$$

$$T_R + T_L + T_\delta = \frac{2\alpha}{\omega}\, c_L + \frac{2\alpha}{\omega}\, c_R + T_\delta = \frac{l_x\, w_p\, (h_L + h_R)}{2\, f} \tag{17}$$

$$c_L, c_R, T_\delta \geqslant 0 \quad \text{and} \quad c_L, c_R \in \mathbb{N} \tag{18}$$

The parameter r_δ (like T_δ) is the compensation for the discrete values assumed by variables c_L and c_R. Since c_L and c_R are integers, it is not guaranteed that their ratio is equal to h_L/h_R, and r_θ is the value of such discrepancy. The residual parameters r_δ and T_δ should be as small as possible. The solution is found by computing the maximum total number N of half-sweeps from Eq. (17) (with $T_\delta = 0$) and, then, by finding the best approximation of the left side of Eq. (16).

Algorithm 1: Compute sweeping pattern on single sector.

Input: h_L, h_R, l_x, w_p, f, α, ω
Output: c_L, c_R, $\{\varphi_i(k)\}_k$, $\{\varphi_f(k)\}_k$;

1: $N \leftarrow \left\lfloor \frac{l_x\ w_p\ (h_L+h_R)\ \omega}{4\ f\ \alpha} \right\rceil$;
2: $m \leftarrow \left\lfloor \frac{h_L}{h_L+h_R}\ N \right\rfloor$;
3: **if** $m \geqslant N-1$ **then**
4: $\quad c_L \leftarrow m$, $c_R \leftarrow N - c_L$;
5: **else**
6: $\quad$ **if** $\left|\frac{h_L}{h_R} - \frac{m}{N-m}\right| < \left|\frac{h_L}{h_R} - \frac{m+1}{N-m-1}\right|$ **then**
7: $\quad\quad c_L \leftarrow m+1$, $c_R \leftarrow N - c_L$;
8: $\quad$ **else**
9: $\quad\quad c_R \leftarrow N - m$, $c_L \leftarrow N - c_R$;
10: $\quad$ **end if**
11: **end if**
12: $k \leftarrow 0$, $i_L \leftarrow 0$, $i_R \leftarrow 0$;
13: **while** $i_L < c_L$ **and** $i_R < c_R$ **do**
14: $\quad$ **if** $i_L c_R \leqslant i_R c_L$ **and** $i_L < c_L$ **then**
15: $\quad\quad \varphi_f(k) \leftarrow \alpha$;
16: $\quad\quad i_L \leftarrow i_L + 1$;
17: $\quad$ **else**
18: $\quad\quad \varphi_f(k) \leftarrow 0$;
19: $\quad$ **end if**
20: $\quad$ **if** $i_R c_L \leqslant i_L c_R$ **and** $i_R < c_R$ **then**
21: $\quad\quad \varphi_i(k) \leftarrow -\alpha$;
22: $\quad\quad i_R \leftarrow i_R + 1$;
23: $\quad$ **else**
24: $\quad\quad \varphi_i(k) \leftarrow 0$;
25: $\quad$ **end if**
26: $\quad k \leftarrow k + 1$;
27: **end while**

Given the number of left and right half-sweeps c_L and c_R, the half-sweeps must be distributed over time in sequences $\varphi_i(k)$ and $\varphi_f(k)$. A criterion is to distribute the half-sweeps as equally as possible while the sprinkler is traversing the current sector. Algorithm 1 reports a simple procedure for the computation of the angle delimiters $\varphi_i(i)$ and $\varphi_f(i)$. First, the number N of half-sweeps is computed (line 1) based on Eq. (17). By choosing N to be the nearest integer, we minimize the value of residual time T_δ. Then, the number of left and right half-sweeps c_L and c_R is computed proportionally to the left and right application depths h_L and h_R (lines 2–11). Lines 12–27 evaluate the angle limits $\varphi_i(k)$ and $\varphi_f(k)$ of sprinkler orientation for each interval k. The variables i_L and i_R count the number of executed left and right half-sweeps. A left half-sweep is executed when the ratio i_L/i_R is less than c_L/c_R. Similarly, a right half-sweep is executed when the reciprocal ratio i_R/i_L satisfies the equivalent statement.

5. Simulation

Simulation enables the assessment of expected results of a planned irrigation before its execution on the field. The planning method for sprinkler-based irrigation illustrated in Section 4 operates on average application rate over field sub-regions. However, the simulation of sprinkler water requires a more detailed distribution of water flow on the ground surface, while avoiding detailed fluid dynamic description. The standard model in literature (Ouazaa et al., 2014; Ferreira Borges and Teixeira de Andrade, 2021) focuses on uniform water distribution in all the directions of the sprinkler during irrigation.

We propose to use probability density functions to describe the application rate of the sprinkler on a specific field point. Such probability

Table 1
Parameter values for simulation of the SIME Elektrorain sprinkler.

Parameter	r	κ	μ_{br}	σ_{br}
Value	44.0 m	498.55	26.0	5 m

functions are simply models and are used for deterministic analysis. Given the sprinkler state $\mathbf{q}$, our goal is to evaluate the instantaneous water flow $f(\mathbf{p})$ on each point $\mathbf{p} \in \mathbb{R}^2$ of the field at a given time instant t. Direct observation (Ouazaa et al., 2014; Li et al., 2015) suggests that the water flow is concentrated around a point corresponding to the sprinkler range r in direction q_φ, although water is distributed also on the distance interval $[0, r]$. Moreover, the sprinkler flow is angularly concentrated around the direction q_φ with standard deviation. Instead of Cartesian coordinates, the distribution of application rate is better modeled in polar coordinates $f(\theta, \rho)$. The complete distribution $f(\theta, \rho)$ is defined as the product of a direction distribution $p_\Theta(\theta)$ and a range distribution $p_\mathrm{P}(\rho)$.

The water flow is higher for θ close to the direction q_φ of the sprinkler gun. The *von Mises* distribution is a suitable central distribution for angles defined as

$$p_\Theta(\theta) = \frac{1}{2\pi I_0(\kappa)} \exp\left(\kappa \cos\left(\theta - q_\varphi\right)\right) \tag{19}$$

where κ is the concentration parameter, q_φ is the mean and mode of the distribution and $I_0()$ is the modified Bessel function of order 0. Since the range ρ is a non-negative quantity, we need a distribution defined on non-negative real domain $[0, +\infty[$. We propose to model the sprinkler range ρ using the easily manageable *biased Rayleigh* (Lodi Rizzini et al., 2019) defined as

$$p_\mathrm{P}(\rho) = \frac{1}{\mathrm{K}_{br}} \rho \exp\left(-\frac{(\rho - \mu_{br})^2}{2\sigma_{br}^2}\right) \tag{20}$$

where μ_{br} is the mode, σ_{br} the width parameter, and K_{br} the normalization constant. The values of μ_{br} and σ_{br} can be set s.t. the sprinkler range r is equal to $\mu_{br} + \alpha\sigma_{br}$ where α is set to include most of the area of the distribution (in our simulation $\alpha = 3$). The application rate distribution is given by the product of the angular and range distributions

$$f(\theta, \rho) = f_{sprinkler}\ p_\Theta(\theta)\ p_\mathrm{P}(\rho) \tag{21}$$

where $f_{sprinkler}$ is the constant water volume per time (in m^3/s) supplied by the sprinkler at constant pressure and nozzle size. Table 1 provides the values of the distribution parameters enabling simulation of the Elektrorain sprinkler used in the experiments. The parameters have been either empirically measured, e.g. the range r or σ_{br}, or derived from empirical quantities, e.g. κ is set to yield a field-of-view of approximately 10°.

Simulation uses the model of the application rate $f(\theta, \rho)$ previously described to evaluate the water volume provided to each sub-region of the field. The flow distribution $f(\theta_i, \rho_i)$ is sampled with desired resolution and its coordinates θ_i and ρ_i are converted to Cartesian ones $\mathbf{p}_i$. A water volume $V_i = f(\theta_i, \rho_i)\Delta t$ is attributed to each sample i and to the field sub-region where $\mathbf{p}_i$ belongs to. Such simple procedure allows prediction of irrigation results. The Octave code of the simulation is publicly available.[5]

6. Experiments

This section describes experiments carried out in summer 2021. We describe the experimental setup including devices, facilities, configuration parameters and deployment activities. Then, we present the quantitative results about controlled water distribution as measured by a set of water catch cans positioned in the ground. Finally, we discuss the outcome of the experiments.

[5] https://github.com/Positive-VRI/vri_sprinkler_simulation.

6.1. Experimental irrigation system

The irrigation setup used in the experiments exploits the POSITIVE information services described in Section 2, where a VRI prescription map is produced by the IRRIFRAME DSS.

The SIme Elektrorain sprinkler is the main actuator operated in the experiment. The sprinkler was clasped and pulled by a hose reel towing machine (manufactured by RM S.r.l.). The whole system is shown in Fig. 5. The Elektrorain is equipped with a control unit that receives commands via a proprietary communication protocol. The hose reel machine is not remotely controllable and can only tow the sprinkler at uniform speed. Such system allows to test VRI between the left and right sub-sectors of the pulling area, while the average supplied water h_a is constant according to Eq. (7). A fully controllable hose reel machine supporting variable retraction speed and application-level communication could modulate the value of h_a in different segments of the field.

The following Elektrorain features make it suitable for VRI:

- Low latency remote control allowed by 3G connection with proprietary communication protocol. An authorized application can send messages to request the rain gun status or to control its motion, e.g. to change the angular limits or rotation speed.
- Programmable irrigation parameters stored by the control unit. Parameters include the head rotation speed setpoint for a specific angle interval and the angle limits of the sweep motion. Through these parameters, the machine behavior can be programmed for differentiated irrigation during the retraction motion.
- Controlled water distribution and angular speed for different angular sectors with 1 deg resolution.
- Sensors reporting operating condition and machine state, including a Global Navigation Satellite System (GNSS) receiver returning the sprinkler position as well as water pressure and tilt sensors.

For the purpose of the experiment, a control application has been developed to translate the VRI prescription map into low-medium level machine commands based on the Elektrorain custom protocol. The control application implements the discrete modeling defined in Section 3, which is updated by reading the status of the machine (last position returned by GNSS and current orientation angle) with a mechanism based on timed polling. The application can control the behavior of the machine both by changing parameters instantaneously (such as speed and direction of rotation) and by setting sections of programmed executions with their associated duration. The application also provides real-time monitoring of parameters such as the traveled distance and the number of half sweeps performed for each side.

6.2. Experiment setup

Irrigation experiments have been carried out in a test field in Emilia-Romagna (latitude 44.570559, longitude 11.533815) on August 2021 in the time frame 9:00-12:00. Temperature increased from 23° to 30° during the experiment, average humidity was 56%, wind was modest at about 8 km/h with south-east direction. The field width is about 40 m and its length about 105 m, corresponding to an usable agricultural surface of about 4200 m^2. The plot was completely bare at the time of the experiment, since the crop had been harvested days before. Fig. 6 shows the plot overlaid with a schema of the actuators and water catch cans positions. Fig. 6 also displays a prescribed water application depth map, enhanced to highlight the difference between right and left sub-sectors. The different amounts of water prescribed have been chosen to stimulate the dynamics of the irrigation system and are not directly verifiable in the water catch cans due to the short transitions between sectors. An overall picture of the water catch cans distribution is given in Fig. 7.

Fig. 5. Top: The irrigation system used in the experiments. Bottom left: Close-up of the sprinkler. Bottom right: Close-up of the hose reel.

Table 2
Irrigation sectors: approximate length, number of half-sweeps (HS) computed for left and right sub-sectors, target and adapted right-to-left (R-L) sweep ratios.

Sector	Length [m]	Left HS Num	Right HS Num	Target R-L ratio	Adapted R-L ratio
1	32	16	20	1.25	1.25
2	7	0	7	0.00	0.00
3	41	29	18	0.70	0.62
4	0[a]	7	0	∞	∞

[a]Sector 4 was executed after the retreat had terminated.

In farming practice, sprinkler irrigation often starts with the rain gun placed at the opposite side of the field and oriented toward the hose reel to supply water inside the field. After a sufficient area has been covered, the rain gun orientation is set to the standard side as represented in Fig. 6. The experiment avoided this maneuver, since the goal was to verify the correct variability in the general sprinkling of the water, without multi-phase operations. Indeed, the experiment considered only the first 80 m of the plot, just behind the initial position of the rain gun.

The sprinkler model described in Section 3 has been adopted to program the irrigation behavior of the system. Some simplifications have been applied to match the constraints given by the available equipment, chiefly the need to program a fixed retraction speed of the towing machine during irrigation.

In the experiment, the sprinkler has been configured to supply an average water application depth of 15 mm across the whole field. As we have chosen to execute irrigation with constant rotation speed, the different prescribed water volumes are achieved by varying the number of times the rain gun irrigates each sub-sector. The rotation speed has been set to about 1.714 °/s (210 s to complete 360°). Global start and end angles have been set at −90° and +90°, where the reference angle 0° corresponds to the center line in the direction opposite to the towed trolley.

Beside the crosswise partition into left and right halves (20 m wide), the field has also been divided lengthwise into 4 longitudinal sectors as listed in Table 2 and shown in Fig. 8. Sectors 2 and 4 have been added to stress the irrigation plan by completely avoiding water supply respectively on their left and right sides. The target of variable rate irrigation has been expressed by means of the right-to-left (R-L) ratio, i.e. the ratio of the sprinkler half-sweeps on the right and the left sub-sectors. Target R-L ratios of sectors 1 and 3 have been set to 1.25 and 0.7, respectively, but due to quantization the planner computed the values reported in Table 2.

In the experiment, the operating pressure measured at the hose reel machine was approximately 4.4 *bar* whereas the average flow rate was about 675 l/min. Considering the average water need of 15 mm, the retraction speed of the rain gun was set to 31 m/h (about 8.61 mm/s). The initial position of the Elektrorain was about 80 m away from the hose reel, reaching approximately the beginning of the plot. The range of the sprinkler jet was empirically estimated as about 44 m.

Fig. 8 shows the data flow required to obtain an irrigation prescription map, which is then translated into an operational plan for the available irrigation equipment.

6.3. Results

The irrigation plan was executed as previously described. About halfway of the pull (namely, after the gun had traveled the distance of 32 m) the system accomplished a change in the water applied (due to the change of sector). Fig. 9 shows the values of sprinkler orientation angle corresponding to the traveled path and the elapsed time from the initial configuration. The number of half sweeps of the rain gun was computed by the planning system and commanded in real-time to the sprinkler controller to achieve the desired balance of irrigation between the left and right sectors. The simulation model described in Section 5 has been used to compute the expected irrigation output. Fig. 10 shows the water quantities predicted by simulation for each squared portion of the field. The water quantity per sub-sector tends to be slightly overestimated, but it is proportional to the supplied water.

The proposed planning strategy delivers different average amount of water to left and right sectors under the assumption of indefinite longitudinal length of sectors. A catch can measures the amount of

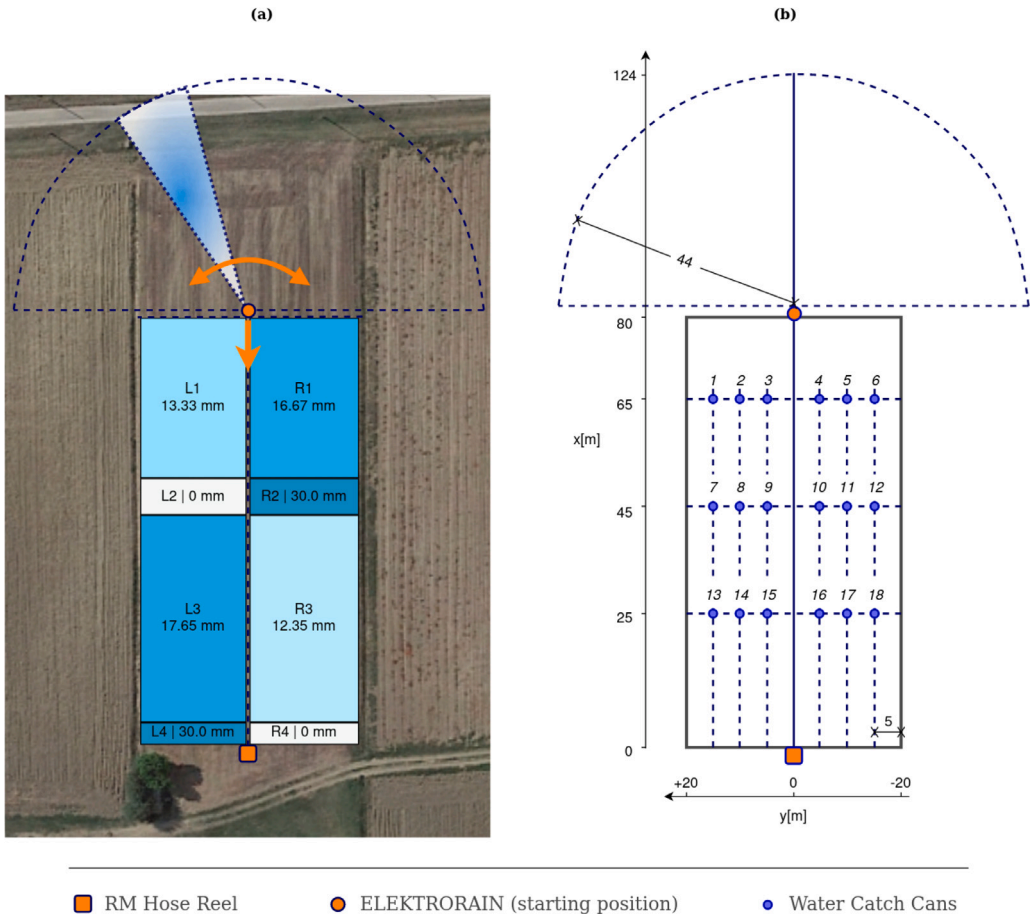

Fig. 6. (a) Plot hosting the sprinkler-based VRI experiment, with sector subdivision and desired water depth. (b) Scheme with the initial positioning of the irrigation system and of the water catch cans. All distances in meters.

Fig. 7. Left: Water catch cans positioned in the plot during the irrigation. Right: Close-up of one of the cans.

delivered water in a given point and collects the overall contribution every time the beam from sprinkler rain gun is directed toward the container. If there are no transitions between longitudinal sectors with different target values, the amount of water collected by the can corresponds to the desired average value for the sector. Otherwise, the collected amount depends on the contributions of multiple sectors.

Fig. 11 reports the water application depths collected in the water catch cans during the experiment, comparing these values with the expected ones. The collected amount of water generally increases from central catch cans (number 3, 4, 9 and 10) to the external ones (number 1, 6, 7 and 12), with the exception of the cans in the final row. This distribution is also discernible in the simulation results in Fig. 10.

Histograms in Fig. 11 also provide the average depth of each left and right half-row of catch cans for comparison with the expected value of the corresponding sector. Water catch cans numbered from 1 to 6 predominantly received water from sprinkler in sector 1 and partially from sectors 2 and 3. Their measured water depths are close to the expected left and right values, in spite of the transitions between

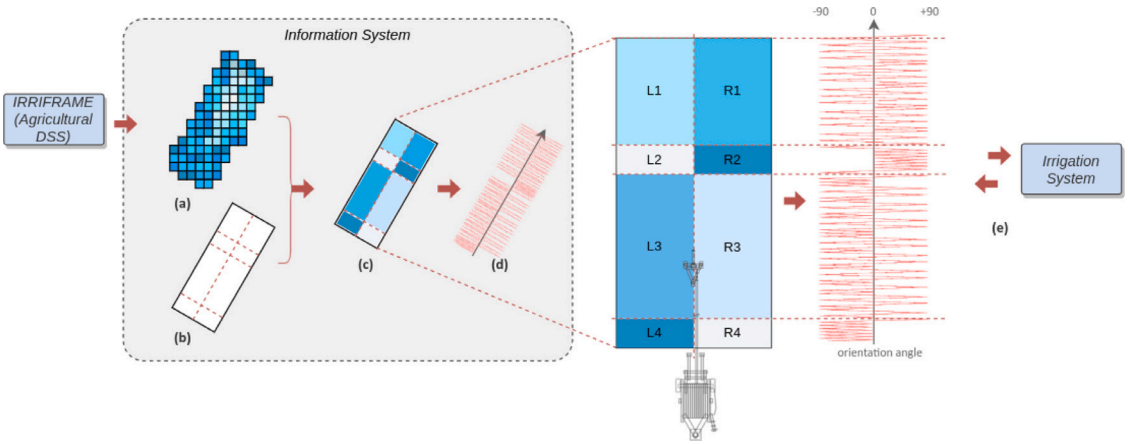

Fig. 8. Data flow to compute a machine-ready irrigation plan suitable for sprinkler operation. The irrigation prescription map is obtained from the IRRIFRAME DSS (a). Using some pre-set parameters (b), based on the characteristics of the irrigation system and of the experiment, an operational irrigation map is computed (c). From the map, an operational plan (d) is derived, which is implemented by the control application and updated based on the feedback (e) of the actuators.

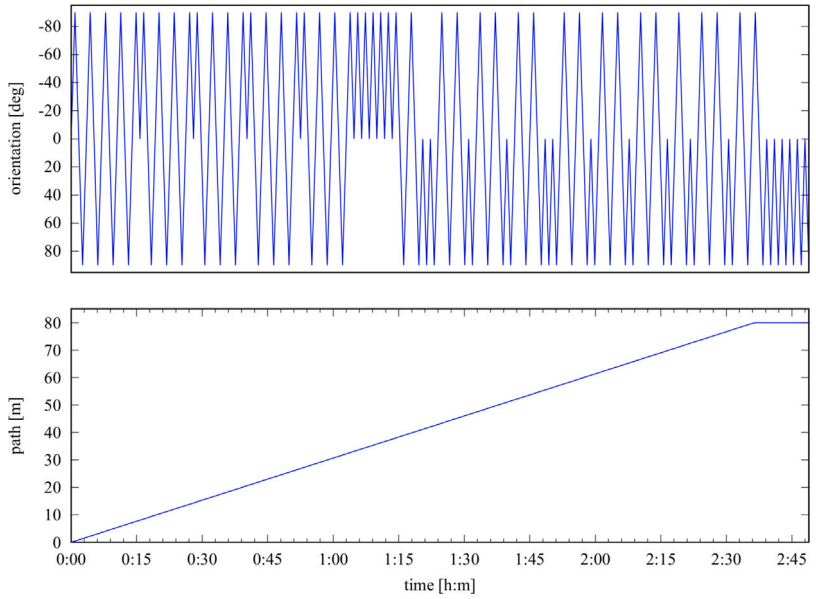

Fig. 9. Orientation angle (top) and traveled path length (bottom) of the rain gun sprinkler with respect to the elapsed time.

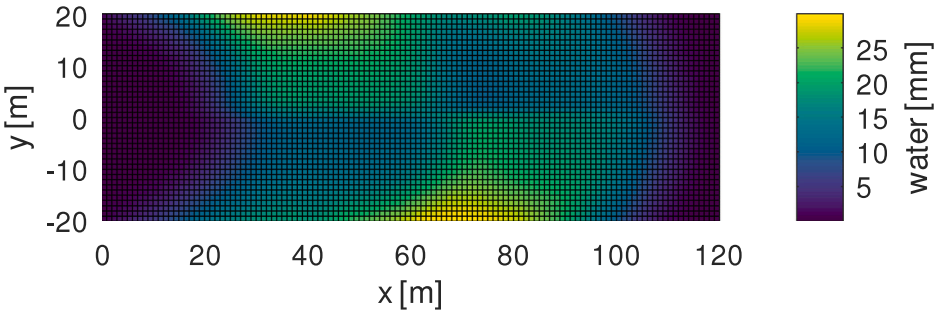

Fig. 10. Results of simulated irrigation using the proposed irrigation model. The resolution of the simulated field is 1 m.

sectors 1 and 2 and between sectors 2 and 3. Water catch cans 7–12 predominantly received water from sprinkler in sector 3, without longitudinal transitions. Hence, their measured depths fairly accurately agree with prescribed left and right average depths, with a maximum error of about 1 mm. Finally, water catch cans numbered from 13 to 18 collected a lower quantity of water (about half of the target values), due to the fact that irrigation was interrupted a few minutes after the trolley had reached the hose reel. However, a partial effect of the longitudinal

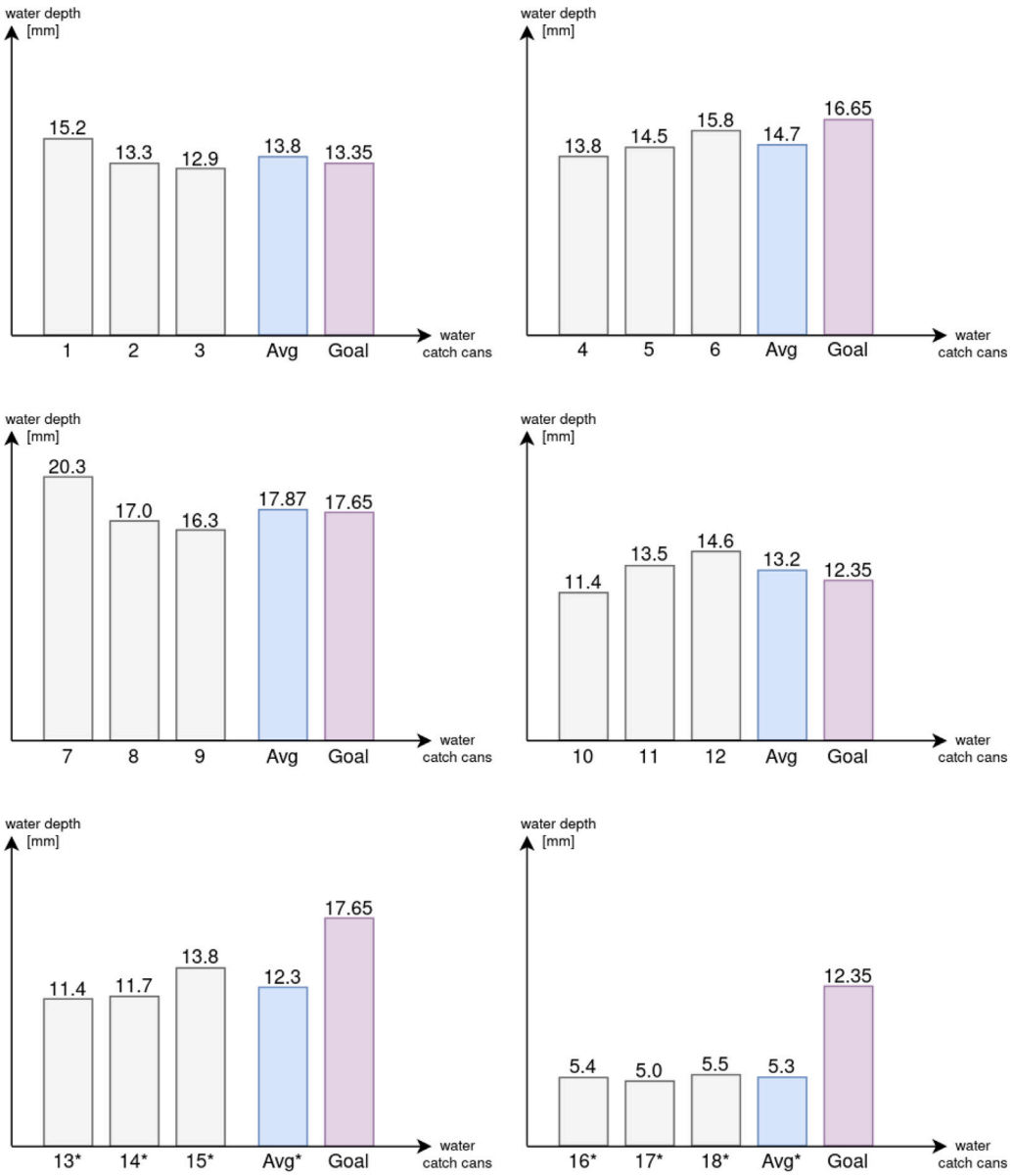

Fig. 11. Histograms representing the quantity of water (in millimeters) measured in water catch cans, corresponding average value (*Avg*), and sector target value (*Goal*), grouped by position. The last group of water catch cans (13 to 18) returned a lower water quantity due to the interruption of the irrigation.

transition between sectors 3 and 4 can be observed in the lower values measured in catch cans 16–18 with respect to catch cans 13–15. In standard practice, irrigation is continued until the desired quantity of water is reached, even if retraction is complete and retraction speed is zero.

As a general remark, the measured application depths values are consistent with the target values when the longitudinal dimension of field sectors is not less than the rain gun range and, thus, there are smooth longitudinal transitions.

7. Conclusions

This paper has reported a method to enable differential irrigation using software-controlled rain gun sprinklers, which can therefore be included among the equipment suitable for advanced VRI application. The proposed irrigation planning algorithm can differentiate the average water application depths supplied to transverse and longitudinal partitions of the field. A field experiment has shown that the application depths measured in specific positions after irrigation are consistent with the expected ones for the sector, under the hypothesis of uniform sprinkler irrigation for the sector and limited longitudinal transitions.

Bringing differential irrigation capabilities to rain gun sprinklers, as proposed in this paper, expands the potential application of VRI, which can lead to major savings of water through the execution of prescription maps consistent with local requirements of the crop (Evans et al., 2020; O'Shaughnessy et al., 2015, 2019).

The applicability of the reported planning algorithm is not bound to the specific machine used, as the underlying model abstracts the technological characteristics common to most rain gun sprinklers. Indeed, the algorithm does not imply particularly advanced machines, requiring only features such as the control of rotation to carry out the differential irrigation.

In future work, we expect to achieve complete VRI capabilities for rain gun sprinklers through the integration of the towing hose reel into the controlled system, in order to exploit the potential of both machines. Furthermore, we plan to extend the model to fully support automated planning of VRI with other linear sprinkling systems such as advanced spray booms (e.g. wing-type booms) and with pivot irrigation systems.

CRediT authorship contribution statement

Gabriele Penzotti: Conceptualization, Methodology, Software, Validation, Writing - original draft, Writing – review & editing. **Dario Lodi Rizzini:** Conceptualization, Methodology, Software, Validation, Writing – original draft, Writing – review & editing. **Stefano Caselli:** Conceptualization, Supervision, Writing – original draft, Writing – review & editing.

Declaration of competing interest

The authors declare that they have no known competing financial interests or personal relationships that could have appeared to influence the work reported in this paper.

Data availability

Data will be made available on request.

Acknowledgments

This research started within the POSITIVE project (ERDF 2014–2020, Research and Innovation of the Region Emilia-Romagna, CUP D41F18000080009) and is currently continued in the frame of the Agritech Spoke 3 National programme.

Funder: Project funded under the National Recovery and Resilience Plan (NRRP), Mission 4 Component 2 Investment 1.4 - Call for tender No. 3138 of 16/12/2021 of Italian Ministry of University and Research funded by the European Union – NextGenerationEU. Award Number: Project code CN00000022, Concession Decree No. 1032 of 17/06/2022 adopted by the Italian Ministry of University and Research, CUP D93C22000420001, "National Research Centre for Agricultural Technologies" (Agritech).

The authors wish to thank SIME S.r.l. and Canale Emiliano Romagnolo for their collaboration in this research.

References

Abioye, E.A., Zainal Abidin, M.S., Azimi Mahmud, M.S., Buyamin, S., Izran Ishak, M.H., Idham Abd Rahman, M.K., Otuoze, A.O., Onotu, P., Azwan Ramli, M.S., 2020. A review on monitoring and advanced control strategies for precision irrigation. Comput. Electron. Agric. (ISSN: 0168-1699) 173, 105441. http://dx.doi.org/10.1016/j.compag.2020.105441.

Adeyemi, O., Grove, I., Peets, S., Domun, Y., Norton, T., 2018. Dynamic neural network modelling of soil moisture content for predictive irrigation scheduling. Sensors (ISSN: 1424-8220) 18 (10), http://dx.doi.org/10.3390/s18103408.

Amoretti, M., Lodi Rizzini, D., Penzotti, G., Caselli, S., 2020. A scalable distributed system for precision irrigation. In: 2020 IEEE International Conference on Smart Computing. SMARTCOMP, pp. 338–343. http://dx.doi.org/10.1109/SMARTCOMP50058.2020.00074.

Bergez, J.E., Leenhardt, D., Colomb, B., Dury, J., Carpani, M., Casagrande, M., Charron, M.H., S. Guillaume, S., Therond, O., Willaume, M., 2012. Computer-model tools for a better agricultural water management: Tackling managers' issues at different scales – A contribution from systemic agronomists. Comput. Electron. Agric. (ISSN: 0168-1699) 86, 89–99. http://dx.doi.org/10.1016/j.compag.2012.04.005.

Brown, M.E., 2015. Satellite remote sensing in agriculture and food security assessment. Procedia Environ. Sci. (ISSN: 1878-0296) 29, 307. http://dx.doi.org/10.1016/j.proenv.2015.07.278.

Carrión, P., Tarjuelo, J., Montero, J., 2001. SIRIAS: a simulation model for sprinkler irrigation. Irrig. Sci. 20 (2), 73–84. http://dx.doi.org/10.1007/s002710000031.

Evans, R.G., LaRue, J., Stone, K.C., King, B.A., 2020. Adoption of site-specific variable rate sprinkler irrigation systems. Irrig. Sci. 31, 871–887. http://dx.doi.org/10.1007/s00271-012-0365-x.

Ferreira Borges, J.C., Teixeira de Andrade, C.L., 2021. Two-dimensional spatial distribution modeling of sprinkler irrigation. Rev. Ceres 68, 257–266. http://dx.doi.org/10.1590/0034-737X202168040002, Vicosa Vol. 68, Issue 4.

Ghinassi, G., 2010. Advanced technologies applied to hose reel rain-gun machines: new perspectives towards sustainable sprinkler irrigation. In: XVIIth World Congress of the International Commission of Agricultural and Biosystems Engineering. CIGR, pp. 1–9.

Haghverdi, A., Leib, B.G., Washington-Allen, R.A., Buschermohle, M.J., Ayers, P.D., 2016. Studying uniform and variable rate center pivot irrigation strategies with the aid of site-specific water production functions. Comput. Electron. Agric. (ISSN: 0168-1699) 123, 327–340. http://dx.doi.org/10.1016/j.compag.2016.03.010.

Hua, L., Jiang, Y., Li, H., Qin, L., 2022. Effects of different nozzle orifice shapes on water droplet characteristics for sprinkler irrigation. Horticulturae 8 (6), 1–15. http://dx.doi.org/10.3390/horticulturae8060538.

Huete, A., Didan, K., Miura, T., Rodriguez, E.P., Gao, X., Ferreira, L.G., 2002. Overview of the radiometric and biophysical performance of the MODIS vegetation indices. Remote Sens. Environ. 83 (1), 195–213. http://dx.doi.org/10.1016/S0034-4257(02)00096-2.

Li, W., Awais, M., Ru, W., Shi, W., Ajmal, M., Uddin, S., Liu, C., 2020. Review of sensor network-based irrigation systems using IoT and remote sensing. Adv. Meteorol. 1–14. http://dx.doi.org/10.1155/2020/8396164.

Li, Y., Bai, G., Yan, H., 2015. Development and validation of a modified model to simulate the sprinkler water distribution. Comput. Electron. Agric. (ISSN: 0168-1699) 111, 38–47. http://dx.doi.org/10.1016/j.compag.2014.12.003.

Lodi Rizzini, D., Galasso, F., Caselli, S., 2019. Geometric Relation Distribution for Place Recognition. IEEE Robot. Autom. Lett. (RA-L) (ISSN: 2377-3766) 4 (2), 523–529. http://dx.doi.org/10.1109/LRA.2019.2891432.

Mannini, P., Genovesi, R., Letterio, T., 2013. IRRINET: large scale DSS application for on-farm irrigation scheduling. Procedia Environ. Sci. (ISSN: 1878-0296) 19, 823–829. http://dx.doi.org/10.1016/j.proenv.2013.06.091.

McCarthy, A.C., Hancock, N.H., Raine, S.R., 2010. VARIwise: A general-purpose adaptive control simulation framework for spatially and temporally varied irrigation at sub-field scale. Comput. Electron. Agric. 70, 117–128. http://dx.doi.org/10.1016/j.compag.2009.09.011.

Miodragovic, R.M, Petrovic, D.V., Mileusnic, Z.I., Dimitrijevic, A.Z., Radojevic, R.L., 2012. Water distribution uniformity of the traveling rain gun. Afr. J. Agric. Res. 7 (13), 1988–1996. http://dx.doi.org/10.5897/AJAR11.810.

Moreira Barradas, J.M., Matula, S., Dolezal, F., 2012. A decision support system-fertigation simulator (DSS-FS) for design and optimization of sprinkler and drip irrigation systems. Comput. Electron. Agric. (ISSN: 0168-1699) 86, 111–119. http://dx.doi.org/10.1016/j.compag.2012.02.015.

Mostafa, H., Derbala, A., 2013. Performance of supplementary irrigation systems for corn silage in the sub-humid areas. Agric. Eng. Int.: CIGR J. 15 (4), 9–15.

O'Shaughnessy, S.A., Evett, S.R., Colaizzi, P.D., 2015. Dynamic prescription maps for site-specific variable rate irrigation of cotton. Agricult. Water Manag. (ISSN: 0378-3774) 159, 123–138. http://dx.doi.org/10.1016/j.agwat.2015.06.001.

O'Shaughnessy, S.A., Evett, S.R., Colaizzi, P.D., Andrade, M.A., Marek, T.H., Heeren, D.M., Lamm, F.R., LaRue, J.L., 2019. Identifying advantages and disadvantages of variable rate irrigation – an updated review. Appl. Eng. Agric. 35 (6), 837–852. http://dx.doi.org/10.13031/aea.13128.

Ouazaa, S., Burguete, J., Pilar Paniagua, M., Salvador, R., Zapata, N., 2014. Simulating water distribution patterns for fixed spray plate sprinkler using the ballistic theory. Span. J. Agric. Res. 12, 850–863. http://dx.doi.org/10.5424/sjar/2014123-5507.

Penzotti, G., Tarasconi, D., Caselli, S., Amoretti, M., 2022. Seamless sensor data acquisition for the edge-to-cloud continuum. In: 2022 IEEE Intl Conf on Pervasive Intelligence and Computing (PiCom). pp. 1–8. http://dx.doi.org/10.1109/DASC/PiCom/CBDCom/Cy55231.2022.9927899.

Pereira, L.S., Gonçalves, J.M., 2018. Surface irrigation. In: Oxford Research Encyclopedia of Environmental Science. Oxford University Press, http://dx.doi.org/10.1093/acrefore/9780199389414.013.248.

Rinaldi, M., He, Z., 2014. Decision support systems to manage irrigation in agriculture. In: Sparks, D.L. (Ed.), Advances in Agronomy. vol. 123, Academic Press, pp. 229–279. http://dx.doi.org/10.1016/B978-0-12-420225-2.00006-6.